J Electr Eng Technol Vol. 8, No. 1: 11-19, 2013
http://dx.doi.org/10.5370/JEET.2013.8.1.011

ISSN(Print) 1975-0102
ISSN(Online) 2093-7423

Analysis of Magnitude and Rate-of-rise of VFTO in 550 kV GIS using EMTP-RV

Hun-Chul Seo*, Won-Hyeok Jang*, Chul-Hwan Kim†, Young-Hwan Chung, Dong-Su Lee** and Sang-Bong Rhee*****

Abstract – Very Fast Transients (VFT) originate mainly from disconnector switching operations in Gas Insulated Substations (GIS). In order to determine the rate-of-rise of Very Fast Transient Overvoltage (VFTO) in a 550 kV GIS, simulations are carried out using EMTP-RV. Each component of the GIS is modeled by distributed line model and lumped model based on equivalent circuits. The various switching conditions according to closing point-on-wave and trapped charge are simulated, and the results are analyzed. Also, the analysis of travelling wave using a lattice diagram is conducted to verify the simulation results.

Keywords: DS, EMTP-RV, Lattice diagram, Rate-of-rise, Travelling wave, Very fast transient overvoltage

1. Introduction

In GIS, VFTOs are generated during the switching operation of a Disconnect Switch (DS) or a circuit breaker. During the switching operation, a number of pre-strikes or re-strikes occur because of the slow speed of the moving contact of DS. These strikes generate VFTO with very high frequency oscillations [1-8]. Even though their magnitudes are lower than Basic Insulation Level (BIL) of the system, they contribute to the aging on the insulation of the system due to their frequent occurrences. Also, VFTO can influence on the insulation of other GIS equipment such as transformers [9-13]. Hence, it is necessary to estimate the magnitudes and the rate-of-rise of VFTO generated during switching operations for insulation coordination of GIS components.

This paper proposes a new method to calculate the rate of rise of VFTO and analyzes the magnitude and rate-of-rise of VFTO at transformer terminals in a 550 kV GIS using EMTP-RV. Firstly, the calculation methods of rate-of-rise are discussed. Secondly, the modelling of each component in GIS is presented. Each component is modelled by distributed line models and lumped line models based on the equivalent circuits recommended by IEEE. Thirdly, the simulations with various switching conditions are performed. The waveform and rate-of-rise of VFTO for each case are presented. The simulation results of rate-of-rise are verified by analysis of travelling wave using a lattice diagram. Finally, all the cases of the rate-of-rise of VFTO according to the simulation conditions are discussed.

† Corresponding Author : College of Information and Communication Engineering, Sungkyunkwan University, Korea (hmwkim@hanmail.net)
* College of Information and Communication Engineering, Sungkyunkwan University, Korea ({hunchul0119, bihyn}@ hanmail.net)
** Power & Industrial Systems PG, Hyosung Corporation, Changwon-city, 641-050, Korea ({gozip, dslee07}@hyosung.com).
*** Dept. of Electrical Engineering., Yeungnam University, Korea (rrsd@yu.ac.kr)
Received: August 8, 2011; Accepted: May 17, 2012

2. Rate-of-Rise of VFTO

The rate-of-rise of VFTO can be defined as the magnitude of voltage per microsecond, i.e. in kV/μs. In this paper, firstly, previous methods to calculate the rate-of-rise of voltage are discussed.

Fig. 1 shows the methods to calculate the rate-of-rise of voltage [14].

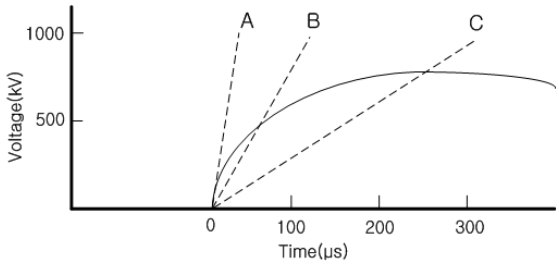

Fig. 1. Methods to calculate rate-of-rise of voltage

In Fig. 1, the rate-of-rise can be calculated as follows:

(1) A: the slope at t=0
(2) B: the average value of method A and method C
(3) C: the slope from t=0 to the first peak voltage

This paper proposes the new method to calculate the rate-of-rise defined in (1). The proposed method uses the second-order difference based on the moving window technique, which is used in transient analysis and protection algorithm of power system. In this paper, a Δt

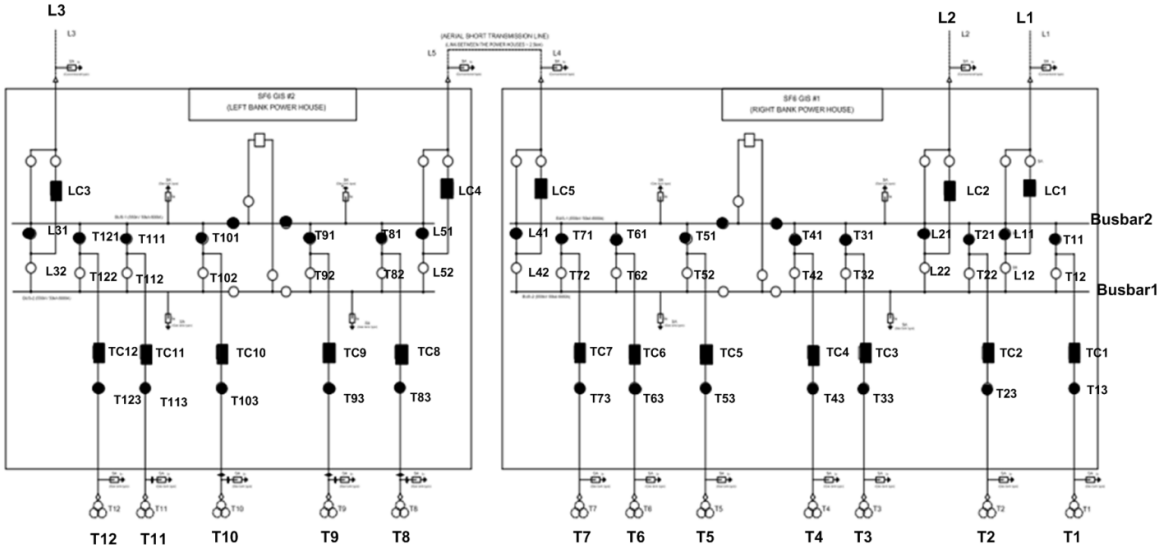

Fig. 2. GIS model

(timestep) is set as 50ns.

$$V_{Rate-of-rise} = \mathrm{Max}\left(\frac{V[i]-V[i-2]}{2\Delta t}\right) \quad (1)$$

Where V[i] and V[i-2] mean the voltage magnitude at present sample and the voltage magnitude of the sample at two times ago.

Since method A and C look at only the beginning part of the VFTO waveform, there is a possibility to miss the maximum rate-of-rise VFTO which may occur after the first peak as the travelling waves arrive. This potential problem can be solved by the proposed method as it takes into account the entire VFTO waveform. By comparing the proposed method with method A and C in Fig. 1, the exact time at which VFTO with the maximum steepness occurs can be found. Also, the magnitude of impulse waveform for field tests can be determined based on (1).

3. Modeling of GIS using EMTP-RV

3.1 GIS model

The GIS in Fig. 2 consists of DS, circuit breakers, earthing switches, feeders connected with transformer (TR feeders), feeders connected with transmission lines (T/L feeders), busbars, coupling feeders, and etc. The rated voltage of GIS is 550 kV. The number of generators connected to transformers is 46 and the capacity of each generator is 83.34MVA. In Fig. 2, L1~L5 indicate the T/L feeders and T1~T12 are the TR feeders. Also, circles signify the DS and rectangles express the circuit breakers. Fig. 2 shows the switching configuration at steady state. The black circles and rectangles illustrate the close state and the white circles and rectangles indicate the open state [15].

3.2 Modelling of each component in GIS

Due to the travelling wave nature of VFTO in a GIS, modelling of the GIS components, such as a busbar, a circuit breaker, and a DS, makes use of electrical equivalent circuits composed of lumped elements and distributed parameter lines. Therefore, this paper performs the modelling of each component using the values recommended by IEEE as shown in Table 1 [1-4].

The parameters such as resistance, surge impedance, and propagation time, of transmission lines, used to model the busbar, the circuit breakers, and the DS, are calculated by EMTP-RV using the geometrical and electrical data of a cable [15-17]. These data are inputted to the distributed line model of EMTP-RV to model the GIS. In case of the circuit breaker, the capacitance of 430pF between each pole is added.

3.3 Modeling of transformer

The modelling of a transformer can be performed by the VFT transformer model as shown in Fig. 3. In this model,

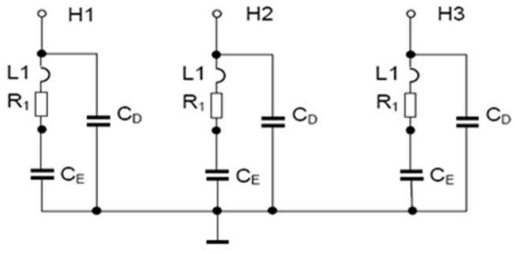

Fig. 3. VFT transformer model

Table 1. Equivalent modeling of GIS components

GIS component	Equivalent model			
Bus bar	Transmission line model (untransposed)			
Circuit Breaker	open state	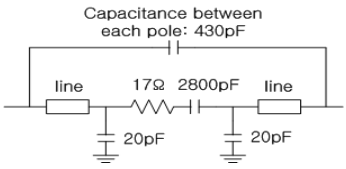	close state	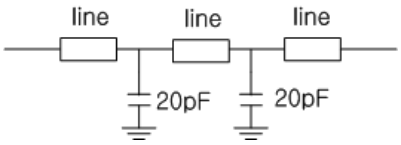
Disconnect Switch	open state	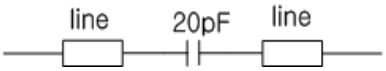	close state	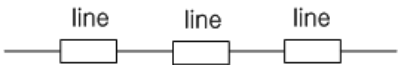
Surge Arrester	Capacitance to ground: 50pF			
Earthing Switch	Capacitance to ground: 45pF			
Bushing	Capacitance to ground: 500pF			

low voltage terminals and neutral are grounded [15].

4. Simulation

4.1 Simulation conditions

This paper conducts the simulation of VFTO occurred by closing a DS at each feeder of Fig. 2. Table 2 shows the simulation conditions. Case 1, 2, 3, 10, and 11 are the cases of closing a DS at the T/L feeder L1, L2, L3, L4 and L5, respectively. Case 4, 5, 6, 7, 8, and 9 are the cases of closing a DS at the TR feeder T1, T4, T7, T8, T10 and T12, respectively. For each case, the simulations according to the various closing points-on-wave and the trapped charge are also performed.

Table 2. Simulation Conditions

Case	Operating Disconnector
Case 1	L11 (LC1 kept open)
Case 2	L21 (LC2 kept open)
Case 3	L31 (LC3 kept open)
Case 4	T11 (TC1 kept open)
Case 5	T41 (TC4 kept open)
Case 6	T71 (TC7 kept open)
Case 7	T81 (TC8 kept open)
Case 8	T101 (TC10 kept open)
Case 9	T121 (TC12 kept open)
Case 10	L41 (LC4 kept open)
Case 11	L51 (LC5 kept open)

4.2 Simulation results

Fig. 4 shows the waveform of the VFTO measured at the transformer T1 when the closing point-on-wave for Case 1 is 90°. The VFTO waveform represents the characteristics of travelling wave and the maximum value of the VFTO is 1.515pu.

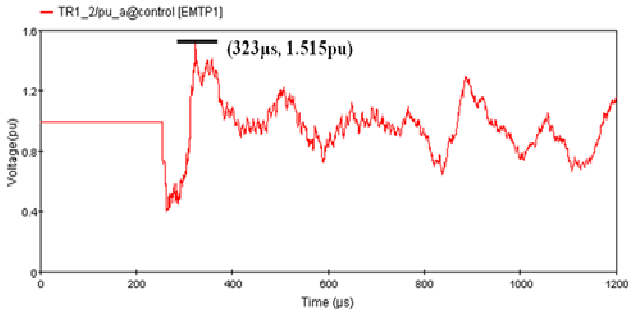

Fig. 4. Waveform of the VFTO measured at the transformer T1 when the closing point-on-wave is 90°

The VFTO is analyzed by using a lattice diagram to verify the simulation results [18, 19]. Fig. 5 shows the result of the VFTO analysis for Case 1 using the lattice diagram. Because many transmission lines between the DS and the transformer terminal have various surge impedances and velocities, the analysis using lattice diagram from t=0 to the simulation time represented in Fig. 4 is impossible. Hence, this paper performs the VFTO analysis using the lattice diagram until the first surge waveform arrives at the transformer terminal. In Fig. 5, α is the reflection coefficient and β is the refraction coefficient. Also, the subscript 1 indicates the direction of the surge wave from the DS toward the transformer terminal and the subscript 2 indicates the direction of the surge wave from the terminal toward the DS. For example, α_{51} and β_{51} mean the reflection coefficient and the refraction coefficient, respectively, for the surge wave at node 5 travelling from the DS to the transformer. As shown in Fig. 5, the rate-of-rise calculated by the lattice diagram analysis for Case 1 is 437.233 kV/μs and this result is very similar to the simulation result. Also, the wave travelling time from the DS to the transformer terminal is 255μs and this result is equal to the simulation result in Fig. 5.

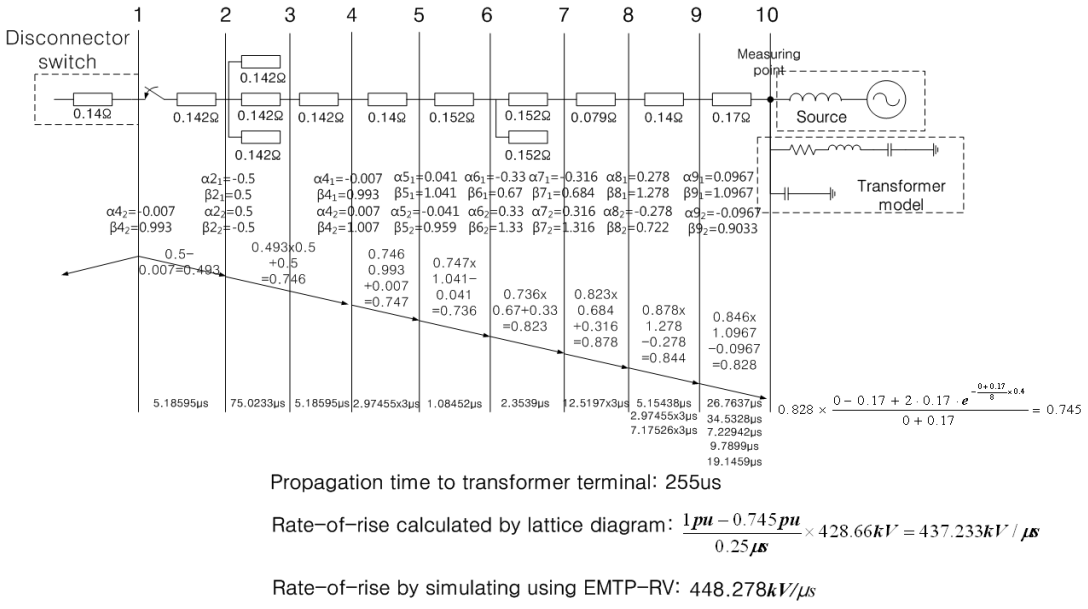

Fig. 5. Verification of Simulation results using lattice diagram for Case 1

4.3 Discussion

4.3.1 Magnitude of VFTO for each case

First, we discuss the magnitude of the VFTO for each case as shown in Fig. 6. The maximum value of the VFTO is 1.515pu in Case 1 and the minimum value of the VFTO is 1.216pu in Case 8. The average value of VFTO for all case in studied system is 1.347pu.

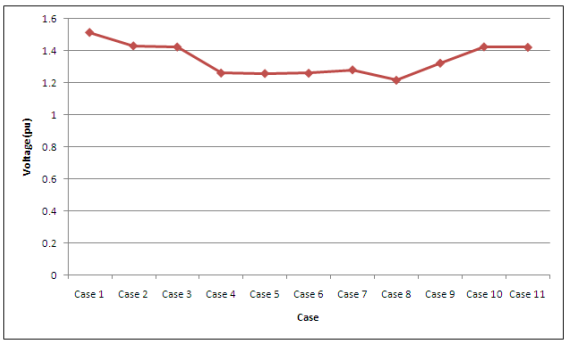

Fig. 6. Magnitude of VFTO for each case

4.3.2 Rate-of-rise of VFTO according to various closing points-on-wave

Fig. 7 shows the rate-of-rise calculated by method A and method C according to the various closing points-on-wave for all cases. As the closing point-on-wave approaches 90° and 270°, the rate-of-rise increases as shown in Fig. 7. On the other hand, as the closing point-on-wave approaches 0° and 180°, the rate-of-rise decreases. The rate-of-rise calculated by method A and C has similar patterns.

Fig. 8 shows the rate-of-rise calculated by proposed method in (1) for all cases. It has a similar trend with Fig. 7.

Table 3 shows the rate-of-rise for each method when the

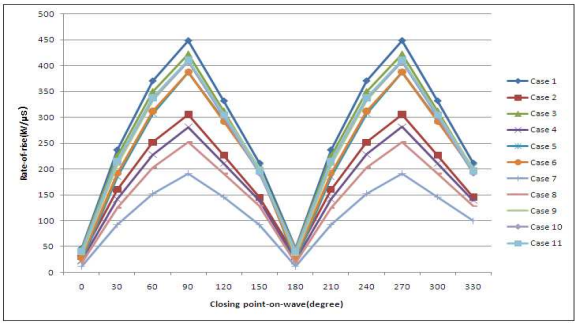

(a) Method A

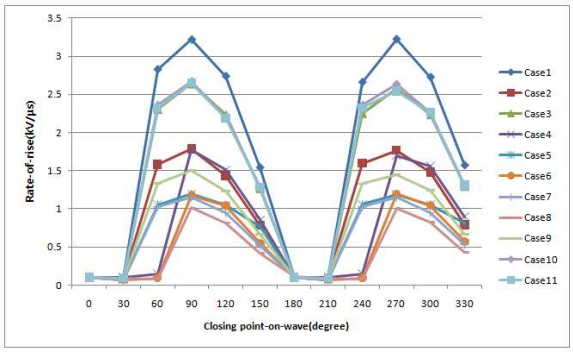

(b) Method C

Fig. 7. Rate-of-rise according to various closing points-on-wave

closing-point-on-wave is 90°. The rate-of-rise calculated by method C is the smallest among three methods. The rate-of-rise calculated by the proposed method is smaller than the one calculated by method A. However, the difference between two values is negligible. Therefore, it indicates that the VFTO with maximum steepness is

occurred when the first surge waveform arrives at the transformer terminal.

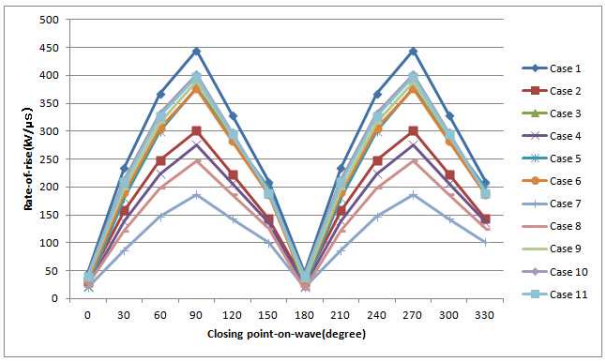

Fig. 8. Rate-of-rise calculated by proposed method

Table 3. Rate-of-rise calculated by each method

	Method A (kV/μs)	Method C (kV/μs)	Proposed Method (kV/μs)
case 1	448.314	3.222	444.24
case 2	305.3	1.786	300.67
case 3	422.87	2.639	400.575
case 4	281.102	1.702	275.384
case 5	387.057	1.191	378.091
case 6	387.52	1.195	376.81
case 7	191.542	1.149	186.934
case 8	252.255	1.009	247.156
case 9	409.691	1.493	389.031
case 10	407.79	2.649	401.623
case 11	410.628	2.649	397.382

4.3.3 Rate-of-rise of VFTO for each case when the closing point-on-wave is equal

Even though simulations are conducted at the same closing points-on-wave in each case, the rates-of-rise of the VFTO are all different from each case as shown in Fig. 7. The reason of this can be explained by two factors; the number of branches on the surge propagation route and the length of propagation route from DS to transformer terminals on surge propagation route.

In Table 4, cases are organized in descending order of rate-of-rise which is calculated by proposed method. The cases in the same row have the same number of branches on the surge propagation route. In case of surge propagation time with 255μs, Case 1 has higher rate-of-rise than Case 2. Also, in case of surge propagation time with 363μs, Case 5, 6 and 9 have higher rate-of-rise than Case 7 and 8. From this result, we can conclude that as the number of branches on the route increases, the rate-of-rise decreases. This can be also verified by the analysis of travelling wave based on the equivalent circuit as shown in Fig. 9.

In Fig. 9, the surge voltage V toward Z_2 is

$$V = \frac{2Z_2}{Z_2 + Z_1} V_1 + \frac{Z_1 - Z_2}{Z_1 + Z_2} V_2 \tag{1}$$

Table 4. Comparison of Simulation Results in Descending Order of Rate-of-rise

Case	Rate-of-rise (kV/μs)	Operating feeder	Branches on surge propagation route and resistance	Surge propagation time from DS to transformer terminal (μs)
1	444.24	T/L	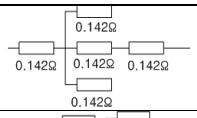	255
3	400.575	T/L	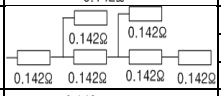	226
11	397.382			240
10	401.623			240
9	389.031	TR	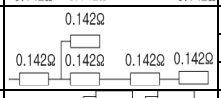	301
6	376.81			363
5	378.091			363
2	300.67	T/L		255
4	275.384	TR	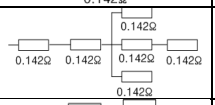	363
8	247.156	TR	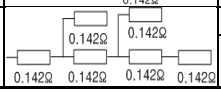	363
7	186.934			363

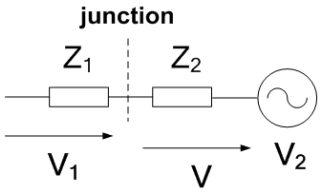

Fig. 9. Equivalent circuit to verify result analysis

First, if we assume V_2=1pu in case of the closing point-on-wave from 0° to 180°, (1) can be written by

$$V = \frac{(2V_1 - 1)Z_2 + Z_1}{Z_2 + Z_1} \tag{2}$$

Let's $2V_1$-1=α, then change of V according to the change of Z_2 by the number of parallel lines is

$$\begin{aligned} \Delta V &= \frac{\alpha Z_2 + Z_1}{Z_2 + Z_1} - \frac{\alpha(Z_2 - \Delta Z_2) + Z_1}{Z_2 - \Delta Z_2 + Z_1} \\ &= \frac{Z_1 \Delta Z_2 (\alpha - 1)}{(Z_2 + Z_1)(Z_2 - \Delta Z_2 + Z_1)} \end{aligned} \tag{3}$$

In (3), the denominator is larger than 0 and $Z_1 \Delta Z_2$ in the numerator is also larger than 0 so that the sign of (3) depends on α-1, i.e. $2(V_1$-1). The magnitude of V_1 is $0<V_1<1$, and hence α-1<0, which means ΔV<0. This result indicates that more branches on the surge propagation route cause a bigger surge voltage and this leads to the lower rate-of-rise as shown in Fig. 10.

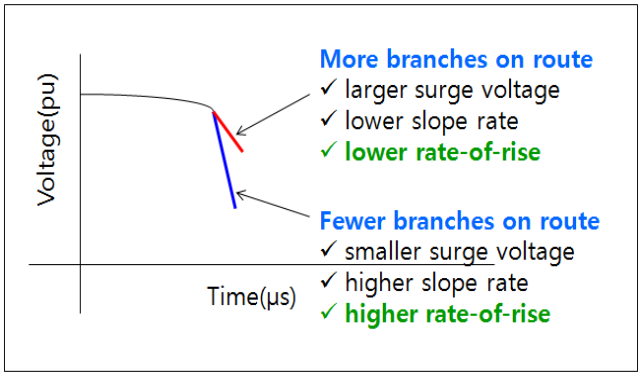

Fig. 10. Relation between rate-of-rise and number of branches on route in case of the closing point-on-wave from 0° to 180°

Second, if we assume V_2=-1pu in case of the closing point-on-wave from 180° to 360°, (1) can be written as

$$V = \frac{(2V_1+1)Z_2 - Z_1}{Z_2 + Z_1} \tag{4}$$

Let's $2V_1+1=\alpha$, then we can find the change of V by the method represented above.

$$\begin{aligned}\Delta V &= \frac{\alpha Z_2 - Z_1}{Z_2 + Z_1} - \frac{\alpha(Z_2 - \Delta Z_2) - Z_1}{Z_2 - \Delta Z_2 + Z_1} \\ &= \frac{Z_1 \Delta Z_2 (\alpha+1)}{(Z_2 + Z_1)(Z_2 - \Delta Z_2 + Z_1)}\end{aligned} \tag{5}$$

In (5), the sign of (5) depends on α+1, i.e. $2(V_1+1)$. The magnitude of V_1 is $-1<V_1<0$, and hence $\alpha+1>0$, which means $\Delta V>0$. This result indicates that more branches on the surge propagation route cause a smaller surge voltage and this leads to the lower rate-of-rise as shown in Fig. 11.

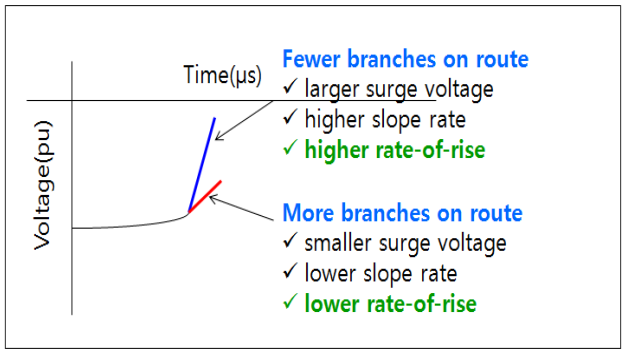

Fig. 11. Relation between rate-of-rise and number of branches on route in case of the closing point-on-wave from 180° to 360°

Also, we can find that the rates-of-rise in Case 1, 3, 10, and 11 are higher than the rates-of-rise in Case 4, 5, 6, 7, 8, and 9. The major difference between the former cases and the latter cases is that the former cases have shorter surge propagation times from the DS to the transformer terminal than the latter cases. Shorter propagation time is derived from the shorter propagation length and the resistances per unit length on the propagation routes are the same. Therefore, shorter propagation time indicates that the route has smaller resistance and vice versa. As the resistance on the route is smaller, the damping of surge also becomes smaller, and consequently, the rate-of-rise becomes higher. Fig. 12 illustrates the relation between the rate-of-rise and the propagation time. This result satisfies regardless of closing point-on-wave.

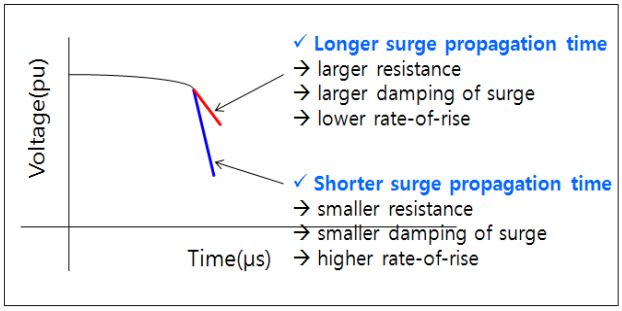

Fig. 12. Relation between rate-of-rise and surge propagation time

There are exceptional cases. Case 9 and 10 does not apply with this result exactly since even though Case 9 has longer surge propagation time than Case 10, the rate-of-rise in Case 9 is lower than one in Case 10. This is because Case 10 has more branches on the surge propagation route than Case 9. Case 2 is also exceptional. Although Case 2 has shorter surge propagation time than Case 9, 6 and 5, the rate-of-rise in Case 2 is lower than Case 9, 6 and 5. This is because it has more branches than Case 9, 6 and 5 so that this fact affected the rate-of-rise to be lower as aforementioned. The exceptional cases do not follow the relation described in Fig. 10, 11 and 12 because the combination of the two factors for the rate-of-rise needs to be considered for those cases. This discussion is based on the rate-of-rise calculated by proposed A. Similarly, the rate-of-rise calculated by method A and C has a same pattern.

4.3.4 Relation between magnitude of first waveform of surge and rate-of-rise according to closing points-on-wave

We compare the maximum rate-of-rise at closing point between 0° and 180° with the magnitude of the first waveform of the surge voltage as shown in Fig. 13. For all cases, the first peak of the surge voltage is less than 0.87pu, which means that the slope of the initial surge voltage for all cases is negative when the closing point is between 0° and 180°. However, since the magnitude of rate-of-rise, not its polarity, is the critical factor, the rate-of-rise is expressed as an absolute value. Therefore, the rate-of-rise

is inversely proportional with the magnitude of the first waveform of the surge voltage when the closing point is between 0° and 180°.

For closing point of between 180° and 360°, on the other hand, the rate-of-rise is proportional with the magnitude of the first waveform of the surge voltage as shown in Fig. 14. This is because the first peak of the surge voltage is bigger than –0.87pu for all cases, which mean that the slope of the initial surge voltage is positive.

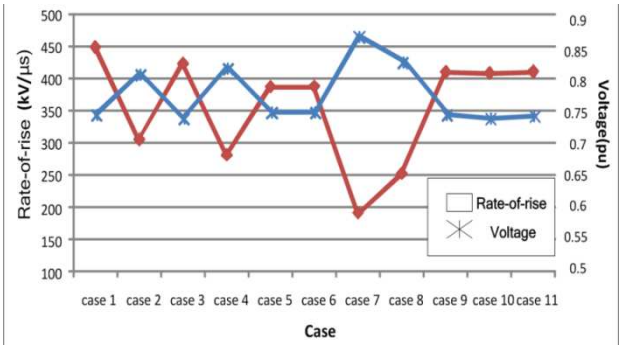

Fig. 13. Relation between the rate-of-rise at closing point between 0° and 180° and the magnitude of the first waveform of the surge voltage

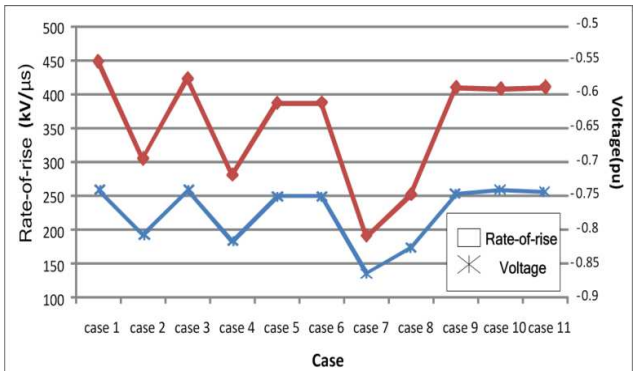

Fig. 14. Relation between the rate-of-rise at closing point between 180° and 360°and the magnitude of the first waveform of the surge voltage

4.3.5 Rate-of-rise of VFTO according to trapped charge

Finally, we discuss the rate-of-rise of the VFTO according to the trapped charge. Fig. 15 shows the rate-of-rise calculated by proposed method for each case. The rate-of-rise remain constantly even with the variation of the trapped charge in all cases. The reason of this result can be discussed using Fig. 16 and 17. Fig. 16 and Fig. 17 show the simplified equivalent circuit for the cases of closing a DS at the T/L feeder (Case 1, 2, 3, 10, and 11) and the cases of closing a DS at the TR feeder (Case 4, 5, 6, 7, 8, and 9), respectively. In Fig. 16 and Fig. 17, the black circles and rectangles illustrate the close state and the white circles and rectangles indicate the open state. In Fig. 16, the section between operating DS and open CB is preloaded, which means charges are trapped within the section. The surge toward the measurement point cannot go into the section of the trapped charge as shown in Fig. 16 and Fig. 17. It means that the first surge waveform measured after closing a DS does not influence on the trapped charge. Therefore, the trapped charge does not influence on the rate-of-rise calculated by proposed method.

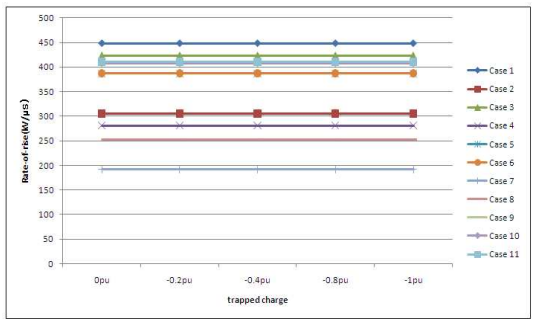

Fig. 15. Rate-of-rise of VFTO according to trapped charge calculated by proposed method

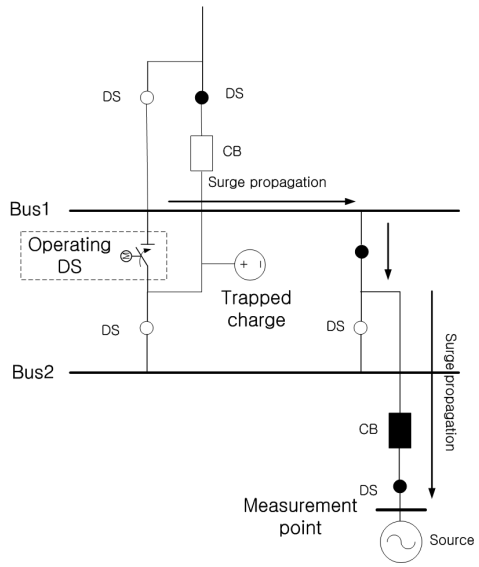

Fig. 16. Simplified equivalent circuit for the cases of closing a DS at the T/L feeder

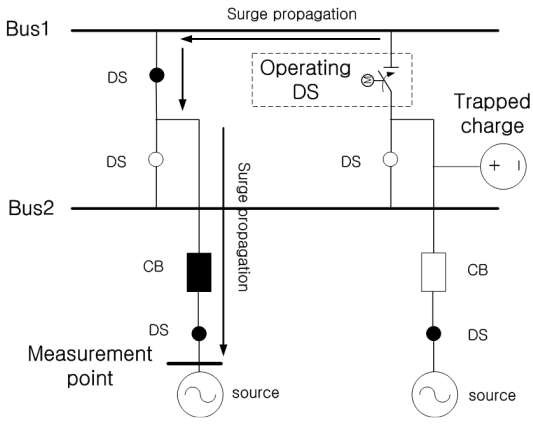

Fig. 17. Simplified equivalent circuit for the cases of closing a DS at the TR feeder

5. Conclusion

In this paper, analysis of the rate-of-rise of VFTO was conducted using EMTP-RV. For GIS components, such as DS, circuit breakers, busbars, and etc., the modeling based on electrical equivalent circuits is performed using EMTP-RV. Also, in case of the transformers, the VFT model given by the manufacturer is used. The various switching conditions were simulated and the simulation results were verified by the lattice diagram. The analysis results can be summarized as follows;

(1) The maximum value of the VFTO measured at the transformer terminal in the studied system is 1.515 pu in Case 1 and the minimum value of the VFTO is 1.216pu in Case 8.
(2) As the number of branches on the surge propagation route is increased, the rate-of-rise is decreased and vice versa.
(3) As the surge propagation length from the DS to the transformer terminal is shorter, the rate-of-rise is increased and vice versa.
(4) As the closing point-on-wave approaches the maximum value of the surge voltage, i.e. 90° and 270°, the rate-of-rise increases, while as the closing point-on-wave approaches the minimum value of voltage, i.e. 0° and 180°, the rate-of-rise decreases.
(5) In case of closing point-on-wave with positive half cycle (from 0° to 180°), the rate-of-rise is inversely proportional with the magnitude of the first waveform of the surge voltage.
(6) In case of closing point-on-wave with negative half cycle (from 180° to 360°), the rate-of-rise is proportional with the magnitude of the first waveform of the surge voltage.
(7) The trapped charge does not influence on the rate-of-rise.

We will study the transient phenomena caused by lightning surge and temporary surge using GIS model presented in this paper.

Acknowledgements

This work was supported by the National Research Foundation of Korea (NRF) grant funded by the Korea government (MEST) (No.2011-0027556).

References

[1] IEEE PES Special Publication, “Tutorial on Modeling and Analysis of System Transients using Digital Programs”, IEEE Working Group 15.08.09, 1998.
[2] D. Povh, H. Schmeitt, O. Volcker, and R. Witzmann, “Modeling and Analysis Guidelines for Very Fast Transients”, IEEE Trans. on Power Delivery, Vol. 11, No. 4, pp. 2028-2035, October, 1996.
[3] J. Meppelink, K. Diederich, K. Feser, W. Pfaff, “Very Fast Transients in GIS”, IEEE Trans. on Power Delivery, Vol. 4, No. 1, pp. 223-233, January, 1989.
[4] V. Vinod Kumar, Joy Thomas M., M.S. Naidu, “Influence of Switching Conditions on the VFTO Magnitudes in a GIS”, IEEE Trans. on Power Delivery, Vol. 16, No. 4, pp. 539-544, Oct., 2001.
[5] A. Tavakoli, A. Gholami, A. Parizad, H. M. Soheilipour, H. Nouri, “Effective Factors on the Very Fast Transient Currents and Voltages in the GIS”, IEEE Transmission & Distribution Conference & Exposition: Asia and Pacific, 2009.
[6] Q. Liu, “Study of Protection of Transformer from Very Fast Transient Over-voltage in 750kV GIS”, International Conference on
Electrical Machines and Systems, Vol. 3, pp. 2153-2156, 2005.
[7] Tian Chi, Lin Xin, Xu Jianyuan, Geng Zhen-xin, “Comparison and Analysis on Very Fast Transient Overvoltage Based on 550 kV GIS and 800kV GIS”, International Conference on High Voltage Engineering and Application, Chongqing, China, November 9-13, 2008
[8] Qing Liu, Yufeng Zhang, “Influence of Switching Conditions on Very Fast Transient Over-voltage in 500kV Gas Insulated Substation”, International Conference on Electrical Machines and Systems, 2008.
[9] J. Ozawa, T. Yamagiwa, M. Hosokawa, S. Takeuchi, H. Kozawa, “Suppression of Fast Transient Over-voltage during Gas DS in GIS”, IEEE Transactions on Power Delivery, Vol. PWRD-1, No. 4, PP. 194-201, October 1986.
[10] J. Amamathl, D.R.K. Paramahamsa, K. Narasimharao, B.P.Singh, K.D. Shrivastava, “Very fast transient over-voltages and transient enclosure voltages in gas insulted Substations”, 2003 Annual Report Conference on Electrical Insulation and Dielectric Phenomena.
[11] D. S. Pinches, M. A. Al-Tai, “Very Fast Transient Overvoltages Generated by Gas Insulated Substations”, International Universities Power Engineering Conference, 2008.
[12] N. Fujimoto, S. A. Boggs, “Characteristics of GIS Disconnector-Induced Short Risetime Transients Incident on Externally Connected Power System Components”, IEEE Transactions on Power Delivery, Vol. 3, No. 3, pp. 961-970, July 1998.
[13] S. A. Boggs, F. Y. Chu, N. Fujimoto, A. Krenicky, A. Plessel, D. Schlicht, “Disconnect Switch Induced Transients and Trapped Charge in Gas-Insulated Substations”, IEEE Transactions on Power Apparatus

and Systems, Vol. 10, No. 10, pp. 3593-3602, October 1982.
[14] Dean E. Perry, Richard C. Raupach, C. A. EDWARD, "A Switching Surge Transient Recording Device", IEEE Trans. on Power Apparatus and Systems, Vol. PAS-87, No. 4, pp. 1073-1078, April, 1968.
[15] Hun-Chul Seo, Won-Hyeok Jang, Chul-Hwan Kim, Toshihisa Funabashi, Tomonobu Senju, "Analysis of rate-of-rise of VFTO according to Switching Conditions in GIS", International conference on Power System Transients 2011.
[16] Hun-Chul Seo, Chul-Hwan Kim, "The analysis of power quality effects from the transformer inrush current: A case study of the Jeju power system, Korea", IEEE Power and Energy Society General Meeting - Conversion and Delivery of Electrical Energy in the 21st Century, 2008.
[17] DCG-EMTP(Development coordination group of EMTP) Version EMTP-RV, Electromagnetic Transients Program. [Online]. Avaliable : http://www.emtp.com.
[18] Allan Greenwood, "Electrical Transients in Power Systems", John Wiley & Sons 1991.
[19] Van der Sluis, "Transients in Power System", John Wiley & Sons 2001.

Hun-Chul Seo He received his B.S and M.S degrees in School of Electrical and Computer Engineering from Sungkyunkwan University, Korea, 2004 and 2006. He worked for Korea Electrical Engineering & Science Institute, Seoul, Korea, as a researcher in power system division from 2006 to 2009. At present, he is working on his Ph. D thesis. His research interests include power system transients, protection and stability.

Won-Hyeok Jang He received his B.S and M.S degree in School of Electrical and Computer Engineering from Sungkyunkwan University, Korea, 2008 and 2010. At present, he is working with Sungkyunkwan University. His research interests include power system transients, protection and stability.

Chul-Hwan Kim In 1990 he joined Cheju National University, Cheju, Korea, as a full-time Lecturer. He has been a visiting academic at the university of BATH, UK, in 1996, 1998, and 1999. Since March 1992, he has been a professor in the School of Electrical and Computer Engineering, Sungkyunkwan University, Korea. His research interests include power system protection, artificial intelligence application for protection and control, the modelling/protection of underground cable and EMTP software. He received his B.S and M.S degrees in Electrical Engineering from Sungkyunkwan University, Korea, 1982 and 1984, respectively. He received a Ph.D in Electrical Engineering from Sungkyunkwan University in 1990. Currently, he is a director of Center for Power IT(CPIT) in Sungkyunkwan University.

Young-Hwan Chung He received his B.S and M.S degrees in School of Electrical Engineering from Pusan National University, Korea, in 1998 and 2000. At present, he has been the manager for reliability engineering team since 2006. His research interest includes power system transients and reliability of high voltage equipments

Dong-Su Lee He received his B.S and M.S degrees in School of Electrical Engineering from Hong-ik University, Korea, in 2004 and 2006. At present, he has been the senior researcher for reliability engineering team since 2007. His research interest includes power system transients and reliability of high voltage equipments.

Sang-Bong Rhee He received his B.S, M.S, and Ph.D. degrees from Hanyang University, Korea, in 1994, 1999, and 2004, respectively. He was a research professor in the School of Electrical and Computer Engineering, Sungkyunkwan University, Korea. Currently, he is an assistant professor with the dept. of electrical engineering at Yeungnam University, Korea. His research interests include a distribution system control and operation, and artificial intelligence applications to power system protection.